Toward the β-$FeSi_2$ *p-n* homo-junction structure

N. Momose [a,b,*], J. Shirai [a], H. Tahara [a], Y. Todoroki [a], T. Hara [a], Y. Hashimoto [b]

[a] *Department of Electrical and Electronic Engineering, Nagano National College of Technology, 716 Tokuma, Nagano 381-8550, Japan*

[b] *Department of Electrical and Electronic Engineering, Faculty of Engineering, Shinshu University, 4-17-1 Wakasato, Nagano 380-8553, Japan*

Abstract

β-$FeSi_2$ thin films were prepared on various substrates, and the influence of the thermal expansion coefficient (TEC) and the softening temperature on the film quality were discussed. It was clarified that a crack-free β-$FeSi_2$ film could be formed on a glass material substrate with a TEC close to that of β-$FeSi_2$, and when the softening point of the substrate is close to the crystal growth temperature of β-$FeSi_2$. A (β-$FeSi_2$) / ($MoSi_2$) / (Corning 1737 glass) stacked structure without leak current was prepared to demonstrate the possibility of a $MoSi_2$ back electrode layer. Furthermore, the (Al-doped *p*-β-$FeSi_2$) / (Ni-doped *n*-β-$FeSi_2$) homo-junction was also prepared by the vacuum evaporation and thermal diffusion method. We have succeeded in achieving current-rectification to a β-$FeSi_2$ thin film, although the anode current was small.

Key words: β-$FeSi_2$, $MoSi_2$, glass substrate, softening temperature, back electrode layer, *p-n* homo-junction

PACS:

1 Introduction

Semiconducting iron disilicide, β-$FeSi_2$ is called "Kankyo (ecologically-friendly) semiconductor", because it is made from ubiquitous and nontoxic materials. β-$FeSi_2$ is expected to be used in optical devices including thin film solar cells, because it has a high absorption coefficient ($\alpha = 10^5$ cm^{-1}, at photon energies higher than 1 eV) and a band gap of approximately 0.85 eV.[1–4] To date, β-$FeSi_2$ has been prepared by various methods.[5–14] However, most films have been prepared on crystalline silicon substrates. In order to use the β-$FeSi_2$ film as a solar cell material, the film should be sufficiently thick and continuous (practically, a thickness of ca. 500 nm is necessary to absorb a luminous flux of 99% when $\alpha = 10^5$ cm^{-1} and the reflectivity is 10%). Moreover, the preparation of films on inexpensive substrates is desirable for applications requiring large area devices.

Herz *et al.* reported that the crack density decreases with a small difference in the thermal expansion coefficient (TEC) between a β-$FeSi_2$ film (6.7×10^{-6}℃$^{-1}$) and a substrate material.[15] However, the melting point of a glass substrate material D-263, with a TEC value close to that of β-$FeSi_2$, is so low and limits the annealing temperature to 500℃. An annealing temperature of more than 800℃ is desirable to obtain a highly crystalline β-$FeSi_2$ film by the simple method of vacuum annealing of Fe-Si evaporated films. Herz *et al.* also reported that films with low crack densities were formed on Corning 7059 glass and sapphire. However, for practical use,

* Corresponding author. Department of Electrical and Electronic Engineering, Nagano National College of Technology, 716 Tokuma, Nagano 381-8550, Japan. Tel: +81 26 295 7066; fax: +81 26 295 4950.

Email addresses: momose@ee.nagano-nct.ac.jp (N. Momose),

hashimt@shinshu-u.ac.jp (Y. Hashimoto).

cheaper substrates than sapphire are necessary.

As previously reported, good quality β-$FeSi_2$ thin films were obtained on 7059 glass substrates by annealing of sputtered Fe-Si precursors at 800℃.[16] After annealing, the substrates were slightly warped (the softening point of 7059 glass is 844℃). It is considered that the stress to the film was decreased by this warping of the substrate during crystal growth. A systematic investigation of the roles of the TEC and the softening of the glass is therefore required.

For use as a thin film solar cell, β-$FeSi_2$ should also be deposited on the back electrode layer. Therefore, when a β-$FeSi_2$ film is prepared on a glass plate for a thin film solar cell, we cannot have electric contact from the back side. The back electrode layer is required to possess a high melting point and not to diffuse into β-$FeSi_2$. $MoSi_2$ is a chemically stable material with a high melting point, and is used as an electrode material in integrated circuits. [17] $MoSi_2$ crystals transform from a semiconducting hexagonal structure to metallic tetragonal structure at approximately 850℃ or more. [18] Therefore, a glass material that can resist high temperature is required for the preparation of tetragonal $MoSi_2$ films.

A *p*-*n* junction should be formed in the β-$FeSi_2$ film in order to obtain the necessary properties for a photovoltaic device. There are very few reports regarding the *p*-*n* homo-junction of β-$FeSi_2$, although hetero-junctions of β-$FeSi_2$ with InP or Si-wafer have already been reported. [19]

In this study, we report on the (1) clarification of the conditions of a low cost substrate material for the preparation of good quality β-$FeSi_2$ continuous films, (2) preparation of a (β-$FeSi_2$ absorber layer) / ($MoSi_2$ back electrode layer) / (glass substrate) stacked structure, and (3) formation of the *p*-*n* homo-junction in a β-$FeSi_2$ film.

2 Experimental

The substrates used in this study are shown in Table 1. The substrates were washed by organic solvent under ultrasonic vibration. Fe-Si, or Mo-Si alloy precursors were deposited using RF-magnetron sputtering equipment. As a sputter target, a 4 sector (80 mm ϕ, 15 degree central angle) Fe or Mo plate[16] (4N, 0.5 mm thick) was placed on a Si-disk (5N, 80 mm ϕ). Si:Fe or Si:Mo ratios of the sputtered films were approximately 2:1, as confirmed by X-ray photoelectron spectroscopy. The thickness of the each deposited precursor was approximately 800 nm. The sputtered samples were sealed in vacuum-ampules (ca. 0.01 Pa), and annealed for 10 hours. After annealing, the samples were cooled naturally to room temperature (RT). In this study, indium tin oxide capping films[16,20,21] were not deposited onto the precursors. X-ray Diffraction (XRD) analysis was used for material identification and evaluation of crystalline properties (θ-2θ scan, 80 mW-CuKα ray). Scanning electron microscopy (SEM) was used for cross-sectional observations and film thickness measurements. The film surfaces were observed using a laser microscope. Optical absorption spectra of the β-$FeSi_2$ samples were measured at RT using a spectrophotometer with a transmission configuration. The four-probe method, thermal probe method, and van der Pauw method were employed for characterization of the electrical properties. The van der Pauw measurement was performed at RT, and the applied magnetic field was 0.7 T. The leak current and current-voltage characteristics were measured using a scanning probe microscope (SPM) and semiconductor characterization system (Keithley, 4200-SCS), respectively.

3 Results and Discussion

3.1 Selection of substrate material

3.1.1 Thermal expansion coefficient

The samples were annealed at a temperature at which all the substrates do not warped (650℃), and the TEC dependence on the β-$FeSi_2$ film quality was investigated. XRD patterns showing single phase β-$FeSi_2$ were obtained for all samples, as shown in Fig. 1. No significant crystalline difference was observed for the glass plate.

Laser microscopic images of the film surfaces grown at 650℃ are shown in Fig. 2. Many cracks with spacing of approximately 1 ~ 10 μm were observed for the quartz and 7913 glass samples, which have large differences in the TEC. It is thought that the photo-absorption of these samples were lower than other samples, as shown in Fig. 3, because these films have many cracks. In contrast, only a few cracks were observed for Tempax float glass, 1737 glass, and 7059 glass substrates, which have TEC close to β-$FeSi_2$. No cracks were observed for the sapphire substrates that have a TEC nearest to that for β-$FeSi_2$. It should be noted that surface of the sapphire substrate was not mirror-polished.

The electrical resistivity of β-$FeSi_2$ films on various substrates are plotted as a function of the TEC (open symbols) in Fig. 4. Some of the films on quartz and 7913 glass were found to possess higher resistivities than $10^4\ \Omega \cdot$ cm, which are not plotted in Fig. 4. The resistivity of the film tends to be low when the TEC of the substrate is close to that of β-$FeSi_2$. It is thought that the presence of cracks significantly reduces the conductivity of the films. All β-$FeSi_2$ films prepared in this

study were *p*-type. Two different thicknesses (1.1 mm and 0.5 mm) of 1737 glass that were used displayed film properties that were almost the same.

3.1.2 Softening of substrates

The samples were then annealed at temperatures where the substrates become moderately warped, and the resulting film properties were compared. However, the substrates were destroyed when they were annealed at the softening point temperatures shown in Table 1. Therefore, the annealing temperatures were adjusted to ca. 90% of the softening point (absolute temperature). The adjusted annealing temperatures for Tempax float glass and 7059 glass were 720℃, and 850℃ for the 1737 glass. Quartz, 7013 glass, and sapphire do not warp in the temperature range where only the β-phase exists ($<$ 937℃).

Figure 5 shows a surface image of a β-$FeSi_2$ film grown on 1737 glass that had warped slightly. Both the micrographic image and scanned line of roughness analysis show a smooth β-$FeSi_2$ surface where the crack density is almost 0. No cracks also appeared in the films on Tempax float glass and 7059 glass substrates. As shown in Fig. 4 (closed symbols), the resistivities of the films have been considerably reduced when the substrates were warped. In all samples on warped substrates, the resistivities were $0.3 \sim 10\ \Omega \cdot \mathrm{cm}$, which is comparable to that observed for films on sapphire substrates. The reduced resistivities, in addition to the smooth surface shown in Fig. 5, indicated the role of substrate softening in improving the film quality. Figure 6 shows the Hall mobilities measured by the van der Pauw method at RT. The tendency of the Hall mobility was found to increase when the TEC is close to that of β-$FeSi_2$. Moreover, the mobilities of all films except the quartz sample exceeded 100 $\mathrm{cm}^2/(\mathrm{V} \cdot \mathrm{s})$. However, these high mobilities are much

higher than other reports, which might be due to the existence of both holes and electrons in the films. The Hall mobility of the film on the quartz substrate was very unstable (Hall voltage from the film on 7913 glass was not observed).

However, many voids of approximately 10 μm in diameter often appeared under the film when the 7059 glass was warped, as shown in Fig. 7. The voids occasionally appeared in Tempax float glass and 1737 glass substrates. Moreover, the Hall mobility decreases significantly when excessive softening occurs, as shown by the shaded triangle in Fig. 6.

From the above results, it is thought that 1737 glass is a suitable substrate for the preparation of β-$FeSi_2$ films, because it can be annealed at 800℃ to obtain a smooth and damage-free structure. Annealing at temperatures above 800℃ is also beneficial for the preparation of the back electrode, as described later.

3.2 Formation of $MoSi_2$ thin film

As a back electrode layer, $MoSi_2$ thin films were formed onto glass substrates. Although many cracks were observed from the $MoSi_2$ films prepared on quartz and 7013 glass substrates, smooth $MoSi_2$ surfaces were obtained on 1737 glass substrates.

Figure 8 shows the changes in the XRD patterns and the resistivity of the $MoSi_2$ films when the annealing temperature was changed. When annealed at 600 to 700℃, hexagonal $MoSi_2$ that has a semiconducting characteristic was formed and the intensity of the XRD peaks was very low. In contrast, by annealing at a higher temperature, the XRD peaks from tetragonal $MoSi_2$ were improved, and the resistivity was decreased. Therefore, since 7059 glass and Tempax float glass cannot be an-

nealed at 850℃, it is thought that 1737 glass, which can be annealed at 850℃, is also suitable for the formation of the $MoSi_2$ electrode layer. The XRD peak marked with a star in Fig. 8(a) seems to be due to the glass substrate (SiO_x) This peak was observed for another 1737 glass substrate annealed without any alloy layer.

3.3 β-$FeSi_2$ / $MoSi_2$ / glass stacked layer

A β-$FeSi_2$ / $MoSi_2$ / glass stacked structure that used a $MoSi_2$ film for the back electrode layer was formed using the above parameters to check the feasibility of a $MoSi_2$ back electrode. Mo-Si alloy films were sputter-deposited using same equipment immediately after the Fe-Si alloy films were formed on 1737 glass substrates. These samples were vacuum-annealed at 850℃ for 10 hours. The thickness of both $MoSi_2$ and β-$FeSi_2$ films was approximately 1 μm.

Figure 9 shows a XRD pattern, cross-sectional view of SEM image, and the *I-V* characteristics of the stacked layer. No phases other than β-$FeSi_2$ and tetragonal $MoSi_2$ were found from the XRD pattern. In addition, smooth interfaces and β-$FeSi_2$ surfaces were obtained. The leakage current from the β-$FeSi_2$ film to $MoSi_2$ layer was measured using a SPM. At this time, a bias voltage of 5 V was applied between β-$FeSi_2$ and $MoSi_2$. However, no shunt path was observed, as shown in Figure 10. We have succeeded in preparing a stacked structure which is applicable to thin film devices using a single annealing process.

3.4 β-$FeSi_2$ *p-n homo-junction*

Reversal of the conduction type in β-$FeSi_2$ was attempted using the method of thermal diffusion of an evaporated dopant layer. Resistance heating type evaporation

equipment was used to deposit the dopant layer. Al was used as the dopant in this study. All the β-$FeSi_2$ films mentioned above were *p*-type. Therefore, to create *n*-type β-$FeSi_2$, Ni was also deposited at the same time as the Fe-Si precursor. A Ni-wire ring (4N, 0.5 mm ϕ) was placed on a Fe-Si sputtering target. The Ni composition ratio of the Fe-Si-Ni precursor was adjusted by the diameter of Ni rings. *n*-Type β-$FeSi_2$ was obtained when the Ni amount was adjusted (ca. 4%-Ni was sputtered). *p*-Type β-$FeSi_2$ areas have been formed in the *n*-type β-$FeSi_2$ when a very thin Al layer (30 ~ 50 nm), deposited on the *n*-type β-$FeSi_2$ film, was heated immediately in the vacuum chamber (500℃).

We have obtained current-rectification from the *p*-*n* junction, as shown in Fig. 11, although the current was very small because the lateral conduction of the thin film was measured.

Regarding the β-$FeSi_2$ *p*-*n* homo junction, investigation of a thermoelectric element prepared from β-$FeSi_2$ bulk has been reported by Yamamoto *et*. *al*.[22] However, including the case of a thin film, the *I*-*V* characteristics of a β-$FeSi_2$ *p*-*n* homo junction, like that shown in Fig. 11, has not been reported.

4 Conclusions

It was found that a β-$FeSi_2$ thin film with small cracks was formed on a substrate with a TEC close to that of β-$FeSi_2$. Crack-free β-$FeSi_2$ films were obtained when the substrate was slightly warped. It was also found that 1737 glass is a suitable substrate for the preparation of β-$FeSi_2$ films. Continuous $MoSi_2$ thin films were also obtained on the same substrates. The electrical conductivity and crystallinity of the $MoSi_2$ thin films were improved when annealed at above 800℃. A β-$FeSi_2$ / $MoSi_2$

/1737 glass stacked structure without leak current was prepared to demonstrate the feasibility of $MoSi_2$ as back electrode layer. We have also prepared *p*-type β-$FeSi_2$ areas in a Ni-doped *n*-type β-$FeSi_2$ film using vacuum evaporation and thermal diffusion of Al. Current rectification was confirmed for the β-$FeSi_2$ thin film, although the anode current was small, in the range of nA. We expect this structure could be applicable to thin film devices using β-$FeSi_2$.

Acknowledgment

The authors would like to thank Mr. I. Minemura of Shinshu University for technical assistance.

References

[1] M. C. Bost and J. E. Mahan, J. Appl. Phys. 58 (1985) 2696.

[2] M. C. Bost and J. E. Mahan, J. Appl. Phys. 64 (1988) 2034.

[3] C. A. Dimitriadis, J. H. Werner, S. Logothetidis, M. Stutzmann, J. Weber and R. Nesper, J. Appl. Phys. 68 (1990) 1726.

[4] K. Lefki and P. Muret, J. Appl. Phys. 74 (1993) 1138.

[5] H. Kakemoto, Y. Makita, S. Sakuragi and T. Tsukamoto, Jpn. J. Appl. Phys. 38 (1999) 5192.

[6] K. Akiyama, S. Ohya, H. Takano, N. Kieda and H. Funakubo, Jpn. J. Appl. Phys. 40 (2001) L460.

[7] K. Akiyama, T. Kimura, T. Suemasu, F. Hasegawa, Y. Maeda and H. Funakubo, Jpn. J. Appl. Phys. 43 (2004) L551.

[8] Y. Maeda, T. Fujita, T. Akita, K. Umezawa and K. Miyake, In: S. Coffa, A. Polman, R. Soref (Eds.), Materials and Devices for Silicon-Based Ooptoelectronics, Boston, December 1-5, 1997, Materials Research Society Symposium Proceedings 486 (1998) 329.

[9] D. J. Oostra, C. W. T. Bulle-Lieuwma, D. E. W. Vandenhoudt, F. Felten and J. C. Jans, J. Appl. Phys. 74 (1993) 4347.

[10] C. Lin, L. Wang, X. Chen, L. F. Chen and L. M. Wang, Jpn. J. Appl. Phys. 37 (1998) 622.

[11] N. Hiroi, T. Suemasu, K. Takakura, N. Seki and F. Hasegawa, Jpn. J. Appl. Phys. 40 (2001) L1008.

[12] T. Yoshitake, T. Hanada and K. Nagayama, J. Mater. Sci. Lett. 19 (2000) 537.

[13] H. Udono and I. Kikuma, Jpn. J. Appl. Phys. 41 (2002) L583.

[14] K. Takakura, T. Suemasu, Y. Ikura and F. Hasegawa, Jpn. J. Appl. Phys. 39 (2000) L789.

[15] K. Herz, M. Powalla and A. Eicke, Phys. Status Solidi A 145 (1994) 415.

[16] Y. Okuda, N. Momose, M. Takahashi, Y. Hashimoto and K. Ito, Jpn. J. Appl. Phys. 44 (2005) 6505.

[17] H. Ishihara, In: S. Gonda (Ed.), Applied Handbook of Thin Film Depositions, 1st Edition, NTS Co., Ltd., Tokyo, 1995, p. 48 (in Japanese).

[18] V. E. Borisenko (Ed.), Semiconducting Silicides, Springer-Verlag, Heidelberg, 2000, p. 33.

[19] K. Okajima, C. Wen, M. Ihara, I. Sakata and K. Yamada, Jpn. J. Appl. Phys. 38 (1999) 781.

[20] N. Momose, Y. Hashimoto and K. Ito, Jpn. J. Appl. Phys. 42 (2003) 5490.

[21] N. Momose, M. Takahashi, Y. Hashimoto and K. Ito, Jpn. J. Appl. Phys. 43 (2004) 6994.

[22] J. Yamamoto, Y. Shimizu, S. Otani, K. Shiozaki and K. Sakaki, J. Jpn. Inst. Metals 67 (2003) 555.

List of figure and table captions

β-$FeSi_2$) homo-junction.

Table 1

Substrate Name	Thermal Expansion Coefficient (10^{-7}℃$^{-1}$)	Softning Point (℃)	Price per 1 cm^2 (yen)	Inclusion
Quartz	5	1650	180	— (100%-purity SiO_2)
Corning 7913 Glass	8	1530	145	— (4%-voids are contained)
Schott Tempax Float	33	820	8	B_2O_3, Na_2O/K_2O, Al_2O_3
Corning 1737 Glass	38	975	10	Al
Corning 7059 Glass	47	840	10	Ba, B
Sapphire	77	2050*	18,000	—
(β-$FeSi_2$)	67	—	—	—

*melting point

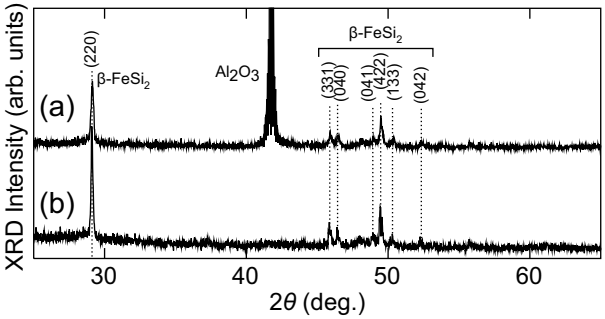
XRD Intensity (arb. units)
(a)
(b)
(220)
β-FeSi2
Al2O3
β-FeSi2
(331)
(040)
(041)
(422)
(133)
(042)
30
40
50
60
2θ (deg.)

Fig. 1.

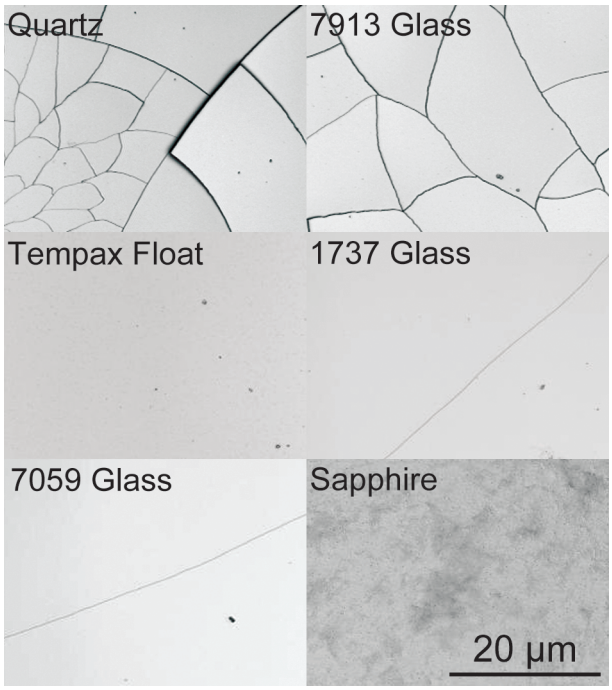
Quartz
7913 Glass
Tempax Float
1737 Glass
7059 Glass
Sapphire
20 µm

Fig. 2.

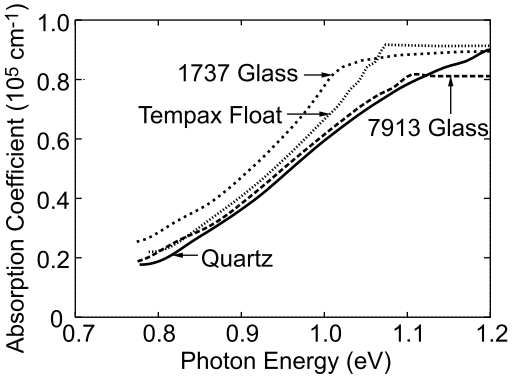
Absorption Coefficient (10^5 cm^{-1})
1.0
0.8
0.6
0.4
0.2
0
0.7
0.8
0.9
1.0
1.1
1.2
Photon Energy (eV)
1737 Glass
Tempax Float
7913 Glass
Quartz

Fig. 3.

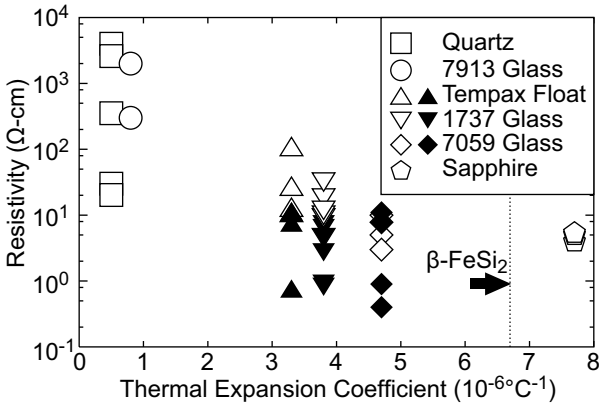
Quartz
7913 Glass
Tempax Float
1737 Glass
7059 Glass
Sapphire
β-FeSi2
Resistivity (Ω-cm)
Thermal Expansion Coefficient (10-6°C-1)

Fig. 4.

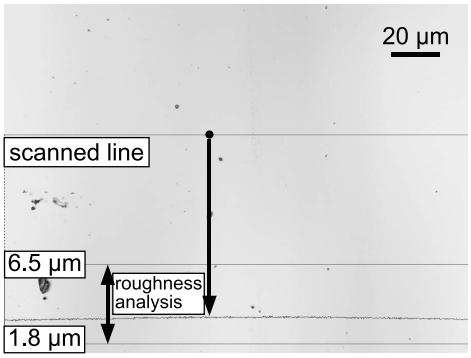

Fig. 5.

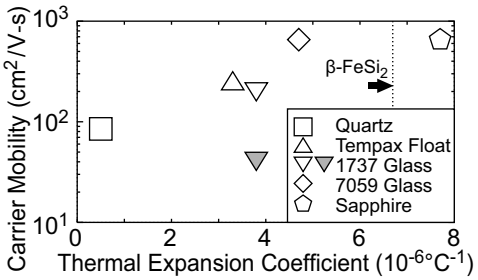
Carrier Mobility (cm²/V-s)
10³
10²
10¹
0
2
4
6
8
Thermal Expansion Coefficient (10⁻⁶°C⁻¹)
β-FeSi₂
Quartz
Tempax Float
1737 Glass
7059 Glass
Sapphire

Fig. 6.

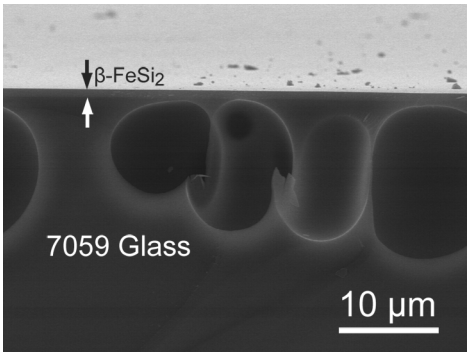

Fig. 7.

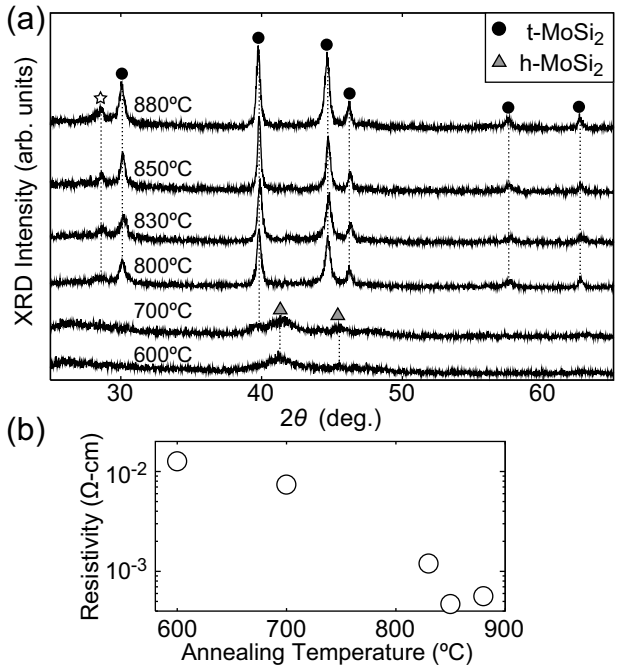
(a)
t-MoSi2
h-MoSi2
880ºC
850ºC
830ºC
800ºC
700ºC
600ºC
XRD Intensity (arb. units)
30
40
50
60
2θ (deg.)
(b)
Resistivity (Ω-cm)
10-2
10-3
600
700
800
900
Annealing Temperature (ºC)

Fig. 8.

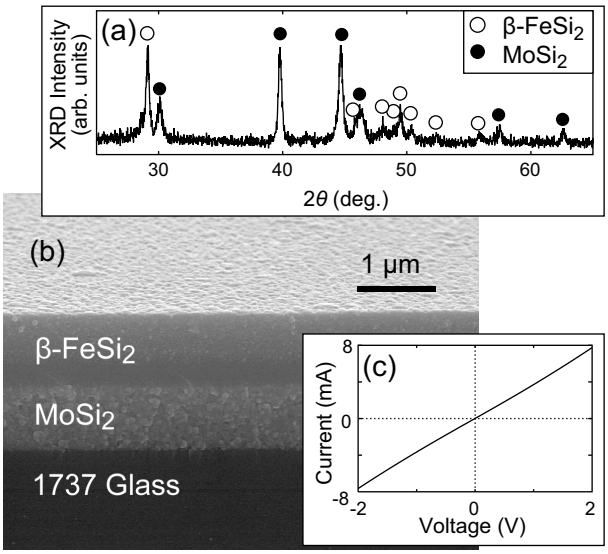
(a)
β-FeSi2
MoSi2
XRD Intensity (arb. units)
30
40
50
60
2θ (deg.)
(b)
1 μm
β-FeSi2
MoSi2
1737 Glass
(c)
Current (mA)
8
0
-8
-2
0
2
Voltage (V)

Fig. 9.

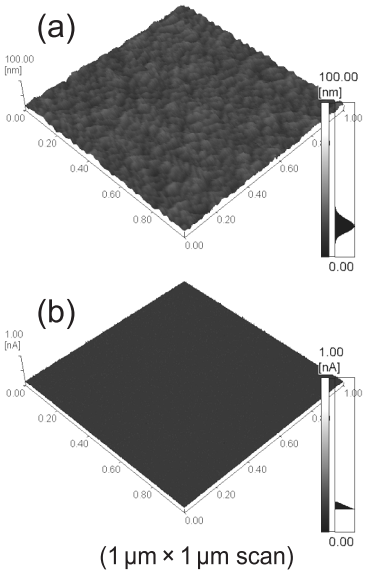

Fig. 10.

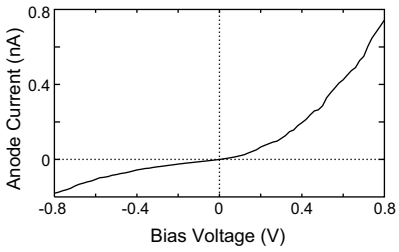

Fig. 11.